MAGNETIC FIELD INFLUENCE ON THE DISCHARGE PARAMETERS OF TWO-STAGE GAS-METAL PLASMA SOURCE

S.V. Shariy, V.B. Yuferov, M.O. Shvets, V.I. Tkachov, V.V. Katrechko

NSC "Kharkov Institute of Physics and Technology", Kharkov, Ukraine

E-mail: v.yuferov@kipt.kharkov.ua

The discharge parameters and vacuum regimes of the two-stage gas-metal plasma source are presented for three configurations of magnetic field. Distributions of deposited flows, current and voltage characteristics of the discharge, current characteristics for reflective electrodes and target are presented. Discharge voltage is 30…150 V, discharge current is up to 25 A. The gas discharge is initiated on air. Vapors of copper were used for discharges in metal. The evaporation rates of copper are obtained at the level of 20…30 g/h. The results of study have shown that mass distribution of flows deposited on the vacuum chamber walls significant deviated from Knudsen-Lamberg`s law described of evaporation in vacuum.

PACS: 52.50. Dg

INTRODUCTION

In article [1] the two-stage gas-metal plasma source project was presented. The requirements to the source were also defined. The possibility of using source for separation technology was considered, in particular for the regeneration of spent nuclear fuel [2]. Sources of this type are widely used in science and technology [3, 4]. They can produce highly ionized flows of plasma with the intensity up to 10 tons per year. Results of the study discharge source parameters are given now. Particular attention is paid to the influence of magnetic field on the discharge parameters. Therefore, in further the operation of the source will presuppose in strong and gradient magnetic fields.

The current and current-voltage characteristics are given for the main discharge and for the reflective electrodes. The analysis of the deposits stream distribution on the walls of vacuum chamber was carried out.

1. SOURCE CONSTRUCTION AND MAGNETIC FIELD CONFIGURATION

Vacuum chamber of source (Fig. 1) is made of nonmagnetic stainless steel and has a diameter of 0.3 m and a length of 0.5 m. The water-cooled anode is made of copper and has a crucible made of tungsten. Reflective discharge electrodes are made of copper and have diameter of 0.2 m. The vacuum system provides the pressure up to $1.3 \cdot 10^{-3}$ Pa. The source has two stages. The nonself-sustained discharge with incandescent cathode in the anode vapors is produces in the primary stage of the source. The primary ionization is carried out here. The reflection discharge (where the degree of plasma ionization is increased and the degree of plasma density is increased) is produced at the second stage.

Discharge voltage is changed from 30 to 150 V, discharge current is up to 25 A. The air was used in the gas discharge. Copper was used for discharges in metal vapors.

The magnetic system consists of two main coils are placed in opposite ends of the vacuum chamber. The additional coil is placed in the lower end of the vacuum chamber. The main coils are connected in series. The current supply is up to 12 A. Additional coil is connected in parallel and opposite with the main coils, the supply current achieved 25 A.

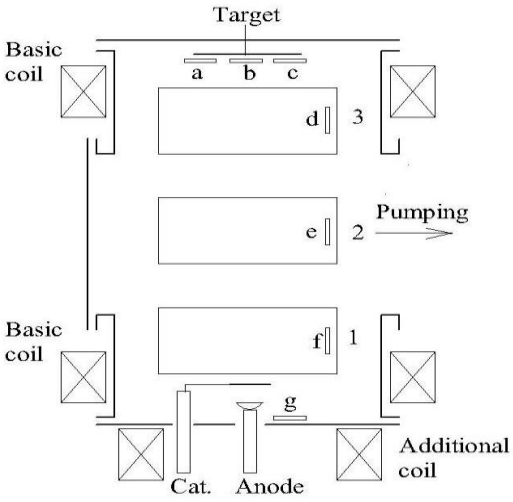

Fig. 1. The scheme of discharge chamber and the magnetic system

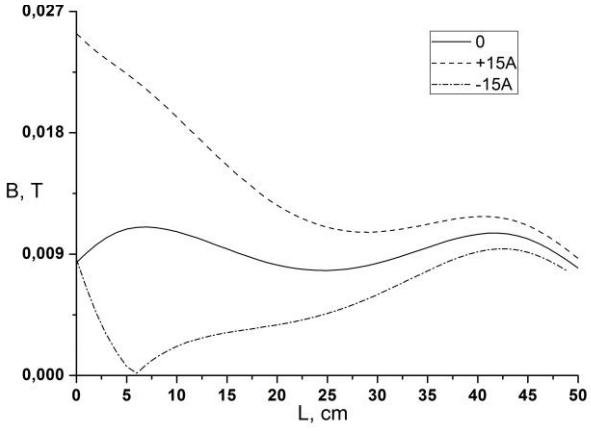

Fig. 2. Axial distributions of magnetic field. The current of main coils is 12 A; the current of additional coil is ± 15 A

Three variants of the magnetic field configuration (Fig. 2) are realized in the experiments. The field of main coils was varied in the first case. The additional coil was connected in series with the main coils in the second case. The additional coil is connected in opposite direction in the third case.

The first case is a trap of symmetrical mirror configuration. The second one is sharply asymmetric trap. For the third case zero field is appeared in anode area.

2. EXPERIMENT RESULTS

Initially, the discharge burns in air (nitrogen). The discharge current can be regulated by the discharge voltage, and the load resistance both. At low discharge currents (up to 6 A), the tungsten crucible is heated not enough for melting of the copper and its effective evaporation. Therefore, the discharge is initiated in the residual gas (nitrogen, oxygen) and has a blue glow. After the increase of the discharge current (>10 A), the copper melts, the discharge acquires a characteristic green color. At that, stage of the discharge current increases under condition of slow increase of the initial voltage. The ionization potential of the copper is lower than the ionization potential of the residual gases (nitrogen, oxygen). The ionization cross section of the gasses is lower. This fact is explained abovementioned discharge current behavior.

The discharge current dependence on the magnetic field induction is shown in Fig. 3. The magnetic field configuration in this discharge is the symmetrical mirror. The discharge voltages are 100 and 120 V. When the magnetic field rise from 0 to $6 \cdot 10^{-3}$ T the discharge current increase is observed. Then, the current slowly increases and goes into saturation at 17 A and 23 A, respectively.

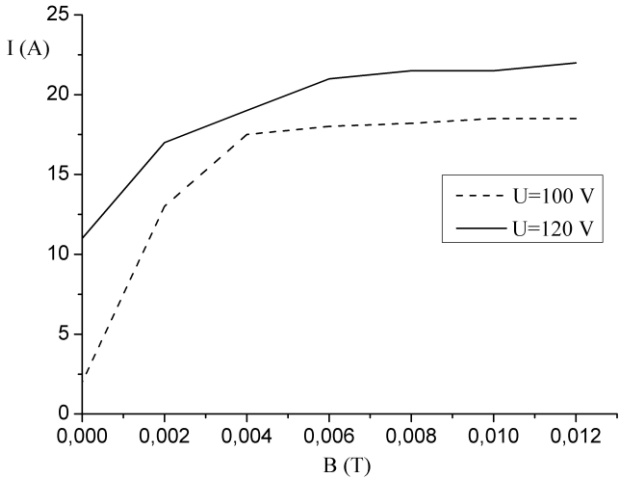

Fig. 3. Dependence of current discharge on the magnetic field

The dependences of discharge currents on the liquid anode − I_d and reflective electrodes − I_1, I_2, I_3 on the voltage across the discharge gap are shown in Fig. 4. The chamber pressure is maintained at $1.3 \cdot 10^{-2}$ Pa. Initially the current increases linearly. The further current increases result in melting of operating metal. The vapors of metal come in the discharge area. The current at the electrodes greatly increases. The discharge takes on a greenish tint glow. It should be noted, that currents I_1, I_2 to the reflective electrodes increase, whereas the current I_3 decreases. Herewith the pressure in the vacuum chamber was set at $2.7 \cdot 10^{-3}$ Pa. Such an effect is often observed in the sputtering installations.

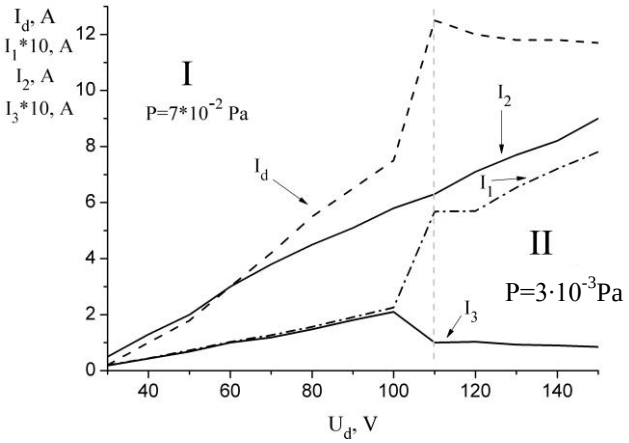

Fig. 4. The discharge current and the currents on the reflective electrode vs. discharge voltage

The dependences of discharge current and current on the target on the discharge voltage are shown in Fig. 5, for the case of a serial ($I_{d,s}$, $I_{t,s}$) and opposite connection of the additional coil ($I_{d,o}$, $I_{t,o}$).

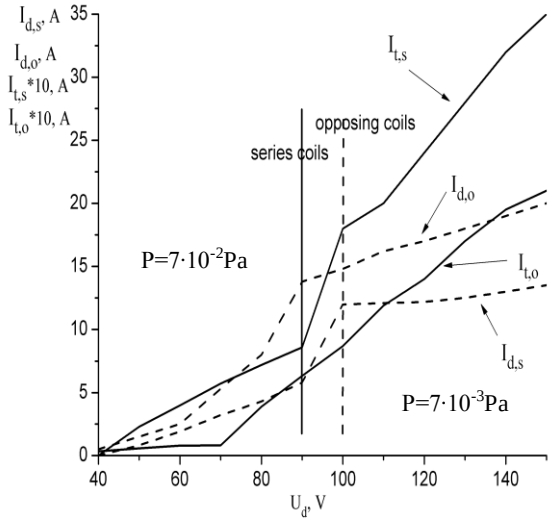

Fig. 5. Discharge current and current on the target vs. discharge voltage for the case of a serial ($I_{d,s}$, $I_{t,s}$) and opposite connection of the additional coil ($I_{d,o}$, $I_{t,o}$). The dashed lines − discharge current, solid lines − current to the target

The target is placed in the opposite from the anode end of the vacuum chamber (see Fig. 1). The transition of the discharge from the gas phase into a discharge in metal vapors stage is shown by the vertical lines. As can be seen, a metal vapor comes earlier in the discharge in the case of opposite connection of the additional coil. We observe higher currents in this case.

The influence of the magnetic field induction and the influence of the additional coil orientation on the discharge current (I_d) and on the current on the target (I_t) are shown in Fig. 6. The current on the target doesn't depend on the direction of the magnetic induction of the additional coil. The current weakly increases with the magnetic induction increasing. The discharge current is higher in the case of opposite connection of the additional coil. It has a characteristic maximum at the additional coil current of 7 A.

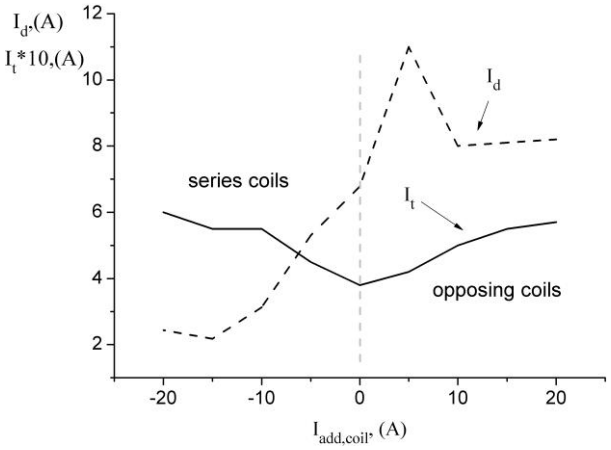

Fig. 6. The discharge current and the current on the target depending on the value and direction of the magnetic field of additional coil. The dashed curve - discharge current, solid curve – current on the target. P=1.3·10^{-2} Pa

3. MASS TRANSFER

The evaporation is not uniform for all directions according to the Knudsen-Lamberg`s law (for the evaporation of the substance in vacuum). The evaporation mainly take place along directions close to the normal surfaces. In the case of vacuum evaporation from a point source at the surface, in the collisionless regime, the weight substance depositing on per unit area in a unit time is:

$$\frac{dM(\alpha,\beta)}{dS} = M_0 \frac{\cos\alpha\cos\beta}{\pi r^2},$$

where α the angle between the vertical to the surface of evaporation and the direction of evaporation, and β the angle between the normal to the surface of the deposition and the direction of evaporation

Then, for the finite size target S_i we have:

$$\Delta M_i = M_0 \frac{S_i \cdot \cos\alpha\cos\beta}{\pi r^2} = M_0 \cdot k_i(S,r,\alpha,\beta),$$

where $k_i(S,r,\alpha,\beta) = \frac{S_i \cdot \cos\alpha\cos\beta}{\pi r^2}$ is a dimensionless factor that depends on the geometrical parameters.

Under conditions of real discharge, we will see a deviation from the Knudsen-Lamberg`s law. This deviation will be more significant under density increasing in the flow and under increasing of the charged particles number in the plasma. The deviation from the low is caused by the charged particles appearance in the discharge and due to the collisionality in the density rising case. The relative deviation and the absolute deviation of deposited mass targets are shown in bar graphs (Figs. 7-9) for the three magnetic field configurations. The depositing targets were placed in a vacuum chamber as shown in Fig. 1, a, b-f).

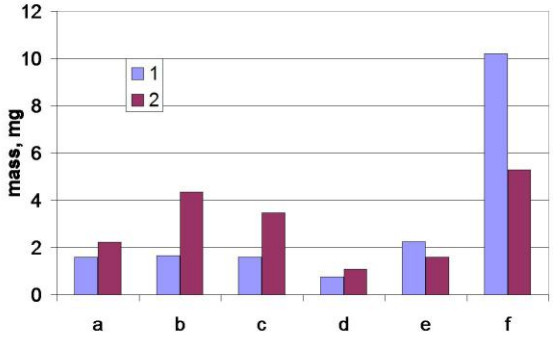

Fig. 7. Mass distribution without additional coil: 1 – theoretical; 2 – real change of the target weight. I_d = 10 A, I_{add} = 15 A, and P = 1.3·10^{-2} Pa

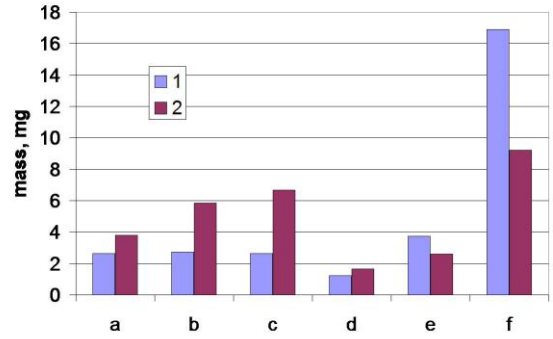

Fig. 8. Mass distribution with the additional coil connected in series with main coils 1 – theoretical; 2 - real change of the target weight. I_d = 10 A, I_{add} = 15 A, and P = 1.3·10^{-2} Pa

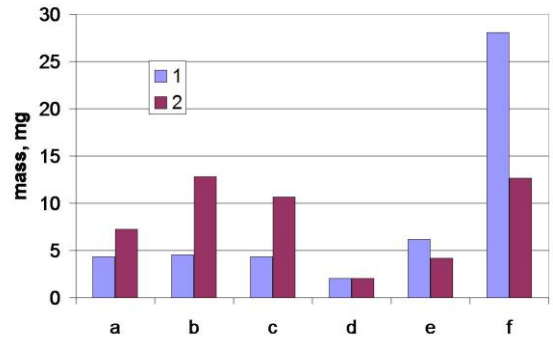

Fig. 9. Mass distribution with additional coil connected in opposite with main coils. 1 – theoretical; 2 – real change of the target weight. I_d = 10 A, I_{add} = -15 A, and P = 1.3·10^{-2} Pa

As can be seen, there is a significant deviation of the mass deposited distribution from the Knudsen-Lamberg`s law for all topographies of the magnetic field. The relative deviation of the mass distribution depends on the magnetic field configuration (Fig. 10).

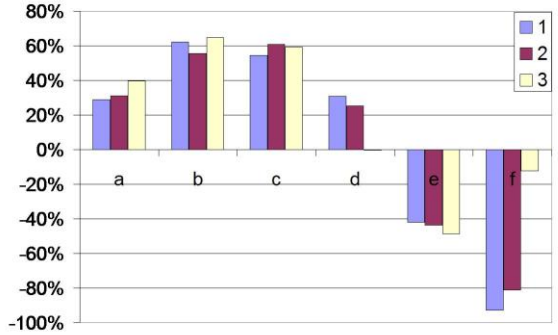

Fig. 10. The percentage deviation of masseas. 1 − without additional coil; 2 − additional coil is connected in series; 3 − additional coil is connected in opposite

CONCLUSIONS

The discharge parameters, burning regimes of vacuum arc and distributions of deposited flows were studied for the three magnetic field configurations. The analysis of distribution of the deposited streams on the vacuum chamber walls were carried out. Itshows a significant deviation of the distribution of masses from Knudsen-Lamberg`s law that describe evaporation in vacuum. It is possible explain by the considerable degree of ionization of the evaporated flow and by the non-ideal source of metal vapor. The depositing layers are metal film with a mirror surface, which is typical for ions deposition. The obtained evaporation rates of copper are from 20 to 30 g/h.

REFERENCES

1. V.B. Yuferov, S.V. Shariy, M.O. Shvets, A.N. Ozerov. Gas-metal plasma source project for the separation technology // *Problems of Atomic Science and Technology*. 2014, № 5(93), p. 184-187.
2. V.B. Yuferov, A.M. Egorov, V.O. Ilichova, S.V. Shariy, K.I. Zhivankov. Plasma separation of spent nuclear fuel one of possible ways to solve a problem of closed fuel cycle // *Problems of Atomic Science and Technology*. 2013, № 2(84), p. 148-151.
3. A.G. Borisenko. The source of macroparticle-free plasma flows for nanoelectronics // *Tekhnologiya i Konstruirovanie v Elektronnoi Apparature*. 2013, № 4, p. 37-41 (in Russian).
4. R.H. Amirov et al. Eksperimentalnoe issledovanie processov vakuumno-dugovogo isparenija i ionizacii veshestva (Gadolinija), modelirujuschego Uran, dla razrabotki technologii plazmennoj separacii otrabotannogo jadernogo topliva // *Trudi MFTI*. 2014, v. 6, № 1, p. 136-145 (in Russian).

Article received 21.10.2016

ВЛИЯНИЕ МАГНИТНОГО ПОЛЯ НА ПАРАМЕТРЫ РАЗРЯДА ДВУХСТУПЕНЧАТОГО ИСТОЧНИКА ГАЗОМЕТАЛЛИЧЕСКОЙ ПЛАЗМЫ

С.В. Шарый, В.Б. Юферов, М.О. Швец, В.И. Ткачёв, В.В. Катречко

Представлены разрядные параметры и режимы горения вакуумной дуги двухступенчатого источника газометаллической плазмы для трёх конфигураций магнитного поля. Приведены распределения осаждаемых потоков, токовые и вольт-амперные характеристики разряда, токовые характеристики для электродов отражательного разряда и мишени. Напряжение разряда 30…150 В, разрядные токи до 25 А. В газовом разряде напускался воздух, для разрядов в парах металла использовалась медь. Полученные скорости испарения меди находятся на уровне 20…30 г/ч. Исследования показали существенное отклонение распределения осаждаемых потоков на стенки вакуумной камеры от закона Кнудсена-Ламберга, описывающего испарение в вакууме.

ВПЛИВ МАГНІТНОГО ПОЛЯ НА ПАРАМЕТРИ РОЗРЯДУ ДВОСТУПЕНЕВОГО ДЖЕРЕЛА ГАЗОМЕТАЛЕВОЇ ПЛАЗМИ

С.В. Шарий, В.Б. Юферов, М.О. Швець, В.І. Ткачов, В.В. Катречко

Наведені розрядні параметри та режими горіння вакуумної дуги двоступеневого джерела газометалевої плазми для трьох конфігурацій магнітного поля. Наведено розподіл осаджуванних потоків, струмові і вольт-амперні характеристики розряду, струмові характеристики для електродів відбивного розряду та мішені. Напруга розряду 30…150 В, розрядні струми до 25 А. У газовому розряді напускали повітря, для розрядів у парах металу використовувалася мідь. Отримані швидкості випаровування міді знаходяться на рівні 20…30 г/год. Дослідження показали істотне відхилення розподілу осаджуваних потоків на стінки вакуумної камери від закону Кнудсена Ламберг, що описує випаровування у вакуумі.